Atmos. Chem. Phys. Discuss., 15, 24871–24908, 2015
www.atmos-chem-phys-discuss.net/15/24871/2015/
doi:10.5194/acpd-15-24871-2015

Atmospheric Chemistry and Physics Discussions
Open Access

Fog composition at Baengnyeong Island in the Eastern Yellow Sea: detecting markers of aqueous atmospheric oxidations

A. J. Boris[1], T. Lee[2], T. Park[2], J. Choi[3], S. Seo[3], and J. L. Collett Jr.[1]

[1]Department of Atmospheric Science, Colorado State University, Fort Collins, 80521, CO, USA
[2]Department of Environmental Science, Hankuk University of Foreign Studies, Yongin, Republic of Korea
[3]Climate and Air Quality Research Department, National Institute of Environmental Research, Incheon, Republic of Korea

Received: 14 August 2015 – Accepted: 20 August 2015 – Published: 11 September 2015

Correspondence to: J. L. Collett Jr. (collett@atmos.colostate.edu)

Published by Copernicus Publications on behalf of the European Geosciences Union.

Abstract

Samples of fog water were collected at Baengnyeong Island (BYI) in the Yellow Sea during the summer of 2014. The most abundant chemical species in the fog water were NH_4^+ (mean of 2220 µM), NO_3^- (1260 µM), SO_4^{-2} (730 µM), and Na^+ (551 µM), with substantial contributions from other ions consistent with marine and biomass burning influence on some dates. The pH of the samples ranged between 3.48 and 5.00, with a mean of 3.94, intermediate within pH values of fog/cloud water reported previously in Southeast Asia. Back trajectories (72 h) showed that high relative humidity (> 80 %) was encountered upwind of the sampling site by all but one of the sampled air masses, and that the fog composition at BYI can be impacted by several different source regions, including the Sea of Japan, Northeastern China, and the East China Sea. Sulfur in the collected fog was highly oxidized: low S(IV) concentrations were measured (mean of 2.36 µM) in contrast to SO_4^{-2} and in contrast to fog/cloud S(IV) concentrations from pollutant source regions; organosulfate species were also observed and were most likely formed through aging of mainly biogenic volatile organic compounds. Low molecular mass organic acids were major contributors to total organic carbon (TOC; 36–69 %), comprising a fraction of TOC at the upper end of that seen in fogs and clouds in other polluted environments. Large contributions were observed from not only acetic and formic acids, but also oxalic, succinic, maleic, and other organic acids that can be produced in aqueous atmospheric organic processing (AAOP) reactions. These samples of East Asian fog water containing highly oxidized components represent fog downwind of pollutant sources and can provide new insight into the fate of regional emissions. In particular, these samples demonstrate the result of extensive photochemical aging during multiday transport, including oxidation within wet aerosols and fogs.

ACPD
15, 24871–24908, 2015

1 Introduction

The chemistry of the atmosphere occurs within multiple phases, one of which is the aqueous phase. Atmospheric water includes fog droplets, cloud droplets, and wet aerosol particles, all of which can act as miniature aqueous reaction vessels. Distinct chemical phenomena occur within the atmospheric aqueous phase: formation of organic hydrates and protonation/deprotonation occur frequently, time spent by reactants in proximity to one another increases, and interactions involving metals such as the Fenton reactions and iron-oxalate complexes are possible (Lelieveld and Crutzen, 1991; Zuo and Hoigné, 1994). The study of carbonaceous species is particularly pertinent to understanding particle, gas, and aqueous phase atmospheric processes because the composition and formation of organics are complex. Particle phase organics in particular cannot yet be modeled well by laboratory or computer experiments (Aiken et al., 2008; Chen et al., 2015; Heald et al., 2005, 2010), and can account for a large fraction of aerosol mass (Fu et al., 2008; Lin et al., 2014; Liu et al., 2012). Uptake of organic components into atmospheric water represents a pathway for removal from the atmosphere, via deposition and/or chemical degradation (Collett et al., 2008). Aqueous atmospheric organic processing (AAOP) can yield low molecular mass products with typically increased volatilities, effectively reducing pollutant concentrations in an air mass via chemical water treatment (Brinkmann et al., 2003; Zhang et al., 2003). Some reactions of organic material within atmospheric water form aqueous secondary organic aerosol (aqSOA) by oxidation of dissolved organic precursors to form lower volatility products that remain in the particle phase as fog drops evaporate (Ervens et al., 2011).

The most common approach to studying AAOP reactions in the lab is to introduce $^{\bullet}$OH oxidant into a bulk solution of a standard carbonaceous "precursor" molecule such as glyoxal and monitor the reactant as it proceeds (Lim et al., 2010). Some assumptions of this common type of simulation can also be studied within a lab: for example, real cloud water constituents have been shown to cause an effective kinetic slowing,

ACPD
15, 24871–24908, 2015

via oxidant competition, of a given organic chemical reaction (Boris et al., 2014). However, while these commonly applied lab simulations are useful for studying specific AAOP reactions, more accurate representations of fogs and clouds are needed to validate simulation results and elucidate more complex phenomena. Daumit et al. (2014) demonstrated that microphysical dynamics of in-droplet diffusion and bidirectional air-water mass transfer are inaccurate in simple "bulk reactions": carrying out a reaction within a photoreactor does not allow species to continuously partition into and out of solution (Ervens et al., 2003). Bulk photoreactions also do not correctly simulate differences in chemical constituents between droplets within a cloud (Bator and Collett, 1997; Collett et al., 1994) gradients inside individual droplets (Ervens et al., 2014), or physical processes of fogs and clouds such as evaporation and deposition (Collett et al., 2008; Herckes et al., 2002; Pandis et al., 1990).

High aerosol concentrations near major cities in China have been attributed in large part to secondary aerosol formation processes and various sources of carbonaceous aerosol (Bian et al., 2014; Zheng et al., 2005). Cloud water collected on Mount Tai in Shandong Province (west of the Yellow Sea) contained some of the highest total organic carbon (TOC) concentrations measured in the world (Herckes et al., 2013; Shen et al., 2012; Wang et al., 2011), consistent with strong regional organic pollutant sources, including agricultural burning (Desyaterik et al., 2013). AAOP reactions could produce measurable quantities of aqSOA and low molecular mass organic acids during atmospheric transport of chemicals, especially at high concentrations and within humid environments as observed in Southeast Asia. Anthropogenic emissions from mainland China and Korea frequently impact remote sites around the Yellow Sea (Kim et al., 2011). Oxygenated organic species observed within atmospheric water and aerosol samples at coastal sites in South Korea (Decesari et al., 2005; Lee et al., 2015) are evidence for AAOP reactions occurring in this part of the world.

Fog water was collected at BYI to characterize the composition of fog formed in aged air masses intercepted in the Eastern Yellow Sea. Frequent sea fog events are observed at BYI, particularly during the late spring and early summer (Cho et al., 2000;

ACPD
15, 24871–24908, 2015

Zhang et al., 2009). In addition to gathering new information about the composition of fogs in this little-studied region, these chemical measurements helped determine whether AAOP reactions occur at BYI, either within the fog or upwind of the sampling site within cloud droplets/wet aerosol particles. It was hypothesized that highly oxidized sulfur and oxidized organics (e.g., low molecular mass organic acids such as oxalic acid) would be measured within the fog water, indicating that AAOP reactions had occurred.

2 Methods

2.1 Study overview

Fog water was collected from 29 June through 21 July 2014 on BYI at an established atmospheric research center (ARC) run by the Korean National Institute for Environmental Research (NIER; 37°58′01″ N, 124°37′48″ E). The collection site was ~ 100 m a.s.l. (Yoo et al., 2010; Zhang et al., 2009) and was collocated with a meteorological station and an international Interagency Monitoring of Protected Visual Environments (IMPROVE) network site. Meteorological data were accessed online (http://rp5.ru/Weather_archive_on_Baengnyeong_Island). The ARC is on the northwest corner of the island; to the east and south are local agricultural sources of emissions and small towns that are home to approximately 4000 total permanent residents. Regular transport of air masses from Eastern China and mainland South Korea were expected to provide a high loading of pollutants to the island (Kim et al., 2006), and frequent haze events were indeed encountered during the study. Three day (72 h) back trajectories generated using the NOAA HySPLIT model (online version: http://ready.arl.noaa.gov/HYSPLIT.php; 0.5° global GDAS archived meteorological data) were used to determine the upwind histories of air masses sampled during fog events. The model was initiated using the coordinates of the research station, a height of 100 m, and the approximate beginning time of each fog event. Latitude,

ACPD
15, 24871–24908, 2015

longitude, and air mass relative humidity (RH) as estimated by the model were outputted at each one-hour interval. Periods during which large-scale fires may have impacted fog samples were detected using MODIS archived graphics retrieved from the Naval Research Lab 7 SEAS Data Repository (http://www.nrlmry.navy.mil/aerosol-bin/7seas/view_7seas_by_date_t.cgi) and NASA FIRMS (produced by the University of Maryland and provided by NASA FIRMS operated by NASA/GSFC/ESDIS; https://earthdata.nasa.gov/earth-observation-data/near-real-time/firms/active-fire-data/).

2.2 Fog collection and handling

A size-fractionating Caltech Active Strand Cloudwater Collector (sf-CASCC; Demoz et al., 1996) was used to collect small and large fog droplets (diameters predominantly 4–16 µm, and > 16 µm, respectively). The sf-CASCC is a polycarbonate structure outfitted with a fan at the rear to pull droplet-laden air into the body of the collector (at 19 $m^3 min^{-1}$). Droplets were impacted onto rows of forward-tilted Teflon rods and strands and pulled by gravity and aerodynamic drag into Teflon sampling troughs at the bottom of the collector. Fog water was collected for durations of one to three hours; four events (1, 2, 5, and 18 July) were long enough for collection of multiple fog samples. A Gerber Particulate Volume Monitor (PVM-100; Gerber, 1991) was used to determine the liquid water content (LWC) of the atmosphere during the study; an approximate threshold of 30 $mg m^{-3}$ was used to initiate fog sampling. When fog was not present, the sf-CASCC inlet and outlet were covered to prevent collection of contaminants onto the inner surfaces of the collector. The sf-CASCC was cleaned after each fog event: a high power sprayer was used to rinse deionized water (~ 2–3 L) through the collector body. Field blanks were collected after each cleaning, and were stored and analyzed in the same manner as samples. Limits of detection (LODs) were calculated using these blanks and are tabulated in Table 1. Deep cleanings were also performed periodically by removing the Teflon strands, rods, and troughs from the body of the sf-CASCC and scrubbing all surfaces with Triton X-100 detergent, then thoroughly rinsing all surfaces

ACPD
15, 24871–24908, 2015

with deionized water. Collected fog water was refrigerated for a short period of time (< 3 h) prior to separation into aliquots for specific chemical analyses.

Contamination from Triton X-100 detergent in the fog water samples between 14 and 19 July and (seven samples) was discovered by positive ionization HR-ToF-MS analysis. TOC concentrations are not reported for the affected samples; however, duplicate analyses of standards of inorganic ions and organic acids containing Triton X-100 were not different from uncontaminated standards. Peroxides, formaldehyde, and S(IV) were also assumed to be unaffected by the contamination.

2.3 Fog water analysis

Samples were each massed, divided into aliquots for analyses, and remaining fog water was stored frozen in Nalgene wide-mouth HDPE plastic bottles (also used for collection). Measurement of fog water pH was carried out at the BYI ARC using a Cole–Parmer microelectrode and pH meter, calibrated with pH 4 and 7 buffers. The mean of three replicate measurements was recorded for each sample. Preservation of other aliquots for chemical analyses (as performed previously; e.g., Benedict et al., 2012) was as follows: peroxides were preserved with *para*-hydroxy-phenyl-acetic acid (POPHA) and ethylenediaminetetraacetic acid (EDTA); S(IV) was stabilized using formaldehyde, *trans*-1,2-cyclohexylenedinitrilo-tetraacetic acid (CDTA) and bovine catalase enzyme added to eliminate hydrogen peroxide; formaldehyde was preserved with Na_2SO_3 and CDTA; samples for analysis of major ionic species (Cl^-, NO_2^-, NO_3^-, SO_4^{-2}, Na^+, NH_4^+, K^+, Mg^{+2}, Ca^{+2}) were aliquotted without added reagents; and microbial activity was eliminated for the storage of organic acids and other organic components by addition of chloroform. Aliquots for TOC and carbohydrates (levoglucosan) analysis were taken from thawed samples after arrival at CSU. Additional organic molecules were identified and/or quantified via high performance liquid chromatography (HPLC) followed by negative electrospray ionization high-resolution time-of-flight mass spectrometry ((-)-ESI-HR-ToF-MS) from the aliquot preserved for organic acids

ACPD
15, 24871–24908, 2015

analysis. Levoglucosan and other carbohydrates were measured using high performance anion exchange chromatography with pulsed amperometric detection (HPAEC-PAD) as described previously (Sullivan et al., 2008).

Deionized water used in analyses and sample collection at BYI was obtained from a distillation and ion exchange/ultraviolet light purification system at the ARC. The calculated charge balance and sample volume were used to determine whether measurements made from a given fog sample were accurate and should be included in results (most samples not containing balanced ionic charges consisted of small liquid volumes). If charge balance, which included all organic and inorganic ionic species, was not within 1.0 ± 0.3 (positive/negative charge), that sample was not included (four of 17 samples were excluded). Directly after sample collection, liquid water from samples with only small collected volumes were dispensed to aliquots according to volume needed and importance of analysis to the study purpose; therefore, in some cases, only some analyses could be carried out for a given sample. For those samples with insufficient volumes (< 2 mL) of the small droplet fraction due to a predominance of large droplets in the sampled fog, the large droplet fraction was assumed to be representative of the entire fog water sample in data analyses. Chemical and physical interactions differ between droplet sizes, and the collection of different sizes of droplets helps preserve real differences in drop composition as compared to bulk fog sampling (Hoag et al., 1999; Moore et al., 2004a, b; Reilly et al., 2001). Mean fog constituent concentrations were calculated from the two droplet fractions (e.g., [(small drop sample volume × small sample concentration) + (large drop volume × large drop concentration)]/total sample volume); mean, median, maximum, and minimum values calculated over the size fraction weighted values of all samples were used in further discussion of the fog chemical composition.

ACPD
15, 24871–24908, 2015

3 Results and discussion

3.1 Fog characteristics and major contributing species

Fog water was collected during nine fog events (17 total samples) at the BYI ARC during July 2014; seven events and 13 samples were included in mean chemical concentrations calculated over the duration of the sampling campaign and will be discussed here (Fig. 1). Events on 2 and 18 July persisted for several hours, allowing collection of up to five samples per event. Air masses sampled during the seven fog events traveled either from the south over the Yellow Sea as documented in Zhang et al. (2009) from the east over the Sea of Japan, or from the north over Northeastern China (Fig. 2). A moderately acidic pH was observed (study mean 3.94, ranging between 3.48 and 5.00). This value is intermediate between values in fog and cloud samples from Southeast Asia (Mount Tai: pH 3.68, Wang et al., 2011; Jeju Island, Korea: pH 5.2, Kim et al., 2006; Daekwanreung, Korea: pH 4.7 Kim et al., 2006; and Shanghai, China: pH 5.97, Li et al., 2011). Major inorganic species contributing to the measured acidity of the fog water at BYI (Table 1; Fig. 3) were NH_4^+ (mean concentration of 2220 µM), followed by NO_3^- (1260 µM), and SO_4^{-2} (730 µM); these concentrations were elevated for fog and cloud samples collected globally (e.g., Collett et al., 2002; Raja et al., 2008; Wang et al., 2011). Sea salt was also an abundant constituent of the fog water (mean concentrations of 551 µM Na^+ and 253 µM Cl^-), as was organic matter (mean 276 µM, estimated using a molecular mass of 100 g mol^{-1} and OM/OC = 1.8; Zhang et al., 2005). The mean NH_4^+ concentration measured at BYI was within the upper range of measured NH_4^+ in fog and cloud samples (similar to e.g., the Po Valley, Italy, Fuzzi et al., 1992; and Baton Rouge, Louisiana, Raja et al., 2008). Although agriculture was a main land use on Baengnyeong Island, no correlation between wind direction and fog NH_4^+ concentrations was observed (Fig. SI-1), suggesting long-range transport of fine particle NH_4^+ as an important source.

ACPD
15, 24871–24908, 2015

3.2 Marine source contribution

Evidence of a marine contribution to fog composition was clear. Upwind trajectories of all air masses sampled included some duration over the Yellow Sea, and in some cases the Sea of Japan (Fig. 2). The study mean Na^+ concentration was 551 µM. Measured Ca^{+2} (study mean 77.4 µM) was contributed in part by sea salt particle scavenging: 21 % was attributed to sea salt (Fig. SI-2) using a molar ratio to Na^+ in seawater of 0.022 (Lee, 2007; Radojevic and Bashkin, 2006). Depletion of particle phase Cl^- appears to have occurred in scavenged sea salt particles, likely due to displacement of HCl to the gas phase by NO_3^- and SO_4^{-2} (Mouri and Okada, 1993). Measured Cl^-/Na^+ molar ratios ranged as low as 0.08, with a mean value of 1.20, which is within measurement error (Table 1) of the typical sea salt ratio of 1.16 (Radojevic and Bashkin, 2006). In some samples, the Cl^- concentration was in excess of the sea salt ratio, indicating possible contributions from other sources such as incineration and coal combustion (McCulloch et al., 1999). Small contributions of K^+ (study mean concentration 82.5 µM) and SO_4^{-2} (study mean concentration 730 µM) were estimated to derive from scavenged sea salt particles: only 12 % of the measured K^+ and 6 % of the SO_4^{-2} were attributed to a marine source on average. Elevated concentrations of cations including K^+ in aerosol have also been associated with the influence of biomass burning activities (Andreae, 1983; Lee et al., 2010), mineral dust from arid regions (Zhang et al., 1993), and/or construction in urban areas (Li et al., 2011).

3.3 Inorganic sulfur

Aqueous sulfur oxidation in the pH range measured in this study (3.48–5.00) is expected to be dominated by reaction with hydrogen peroxide (Rao and Collett, 1995). The mean concentrations of S(IV) and total peroxides (2.36 and 7.8 µM, respectively; Table 1) were low compared to the mean S(IV) and peroxides concentrations measured during summer 2007 and 2008 field campaigns at Mount Tai, China (Shen et al., 2012), consistent with a low potential for additional S(IV) oxidation within the BYI fog

ACPD
15, 24871–24908, 2015

samples (Fig. 4). Since Mount Tai is located west across the Yellow Sea from BYI, and is influenced by the abundant SO_2 sources in Shandong Province including large numbers of coal-fired power plants, these observations are consistent with extensive aging of S(IV) during transport to the BYI fog collection site. In contrast to BYI measurements, cloud samples from the remote Southeastern Pacific, for example, contain high concentrations of peroxides and low concentrations of S(IV) (1.9–610 µM peroxides, < 0.91–3.7 µM S(IV); Straub et al., 2007 and Benedict et al., 2012). Measured SO_4^{-2} was abundant within BYI samples, demonstrating that sources of atmospheric sulfur existed upwind, and that oxidation of sulfur occurred prior to arrival at BYI. Between 98.9 and 99.8 % of sulfur measured (as the sum of SO_4^{-2} and S(IV)) was in the form of SO_4^{-2}. The organic acid methanesulfonic acid (MSA) was observed within all fog samples collected at BYI, indicating that oxidation of marine emissions via either $OH^{\bullet}$ or $NO_3^{\bullet}$ reaction occurred upwind of fog collection at BYI (Seinfeld and Pandis, 2006).

3.4 Total organic carbon

Concentrations of fog water TOC measured at BYI were 3.60–24.8 mg C L^{-1}, with a mean of 15.3 mg C L^{-1}, comparable to concentrations measured in polluted environments globally (Herckes et al., 2013). Although the mean BYI TOC was also similar to that measured in cloud water from Mount Tai during the summer of 2008 (15.8 mg C L^{-1}), several samples impacted by agricultural burning were collected during the latter campaign ranging between 100 and 200 mg C L^{-1} (Shen, 2011).

3.5 Organic acids

The products of AAOP reactions commonly include C_2–C_4 (two to four carbon) oxo- and di-carboxylic acid molecules (Lim et al., 2010). The percent BYI fog TOC accounted for by organic acids was 36–69 % (mean 52 % by mole; $N = 8$), which is at the upper end of values typical for fog samples (e.g., 16 % at Davis, CA, Herckes

ACPD
15, 24871–24908, 2015

et al., 2002; 18 % at Angiola, CA, Ervens et al., 2003; 43 % at Fresno, CA, Collett et al., 2008; 44 % at Baton Rouge, LA, and 51 % at Houston, TX, Raja et al., 2008). Among the organic acids quantified, major contributions to TOC came not only from acetic and formic, but also succinic, maleic and oxalic acids, with lesser but substantial contributions from other acids (Fig. 5). Concentrations of low molecular mass organic acids were strongly correlated with one another (air equivalent concentrations: $r^2 = 0.83$ on average, ranging from 0.47 to 0.99 for C_1–C_6 mono and di-acids). The predominance of succinic acid suggests a major anthropogenic source of organic acids at BYI (Kawamura and Ikushima, 1993). Although oxalic acid in particular has been used as a molecular marker for AAOP reactions (Sorooshian and Varutbangkul, 2006; Wonaschuetz et al., 2012; Yu et al., 2005), other sources for oxalic acid in the atmosphere have been proposed: gas-phase oxidation of aromatic and anthropogenic molecules (Edney et al., 2000; Kamens et al., 2011; Kleindienst et al., 1999; Borrás and Tortajada-Genaro, 2012; Kalberer et al., 2000), diesel exhaust emissions (Kawamura and Kaplan, 1987), and forest fire emissions (Narukawa and Kawamura, 1999; Yamasoe et al., 2000). Thus, while substantial contributions of oxalic acid to TOC suggest that AAOP took place, they are not unequivocal evidence of it. MSA may also be formed mainly in the aqueous phase via reaction with $OH^{\bullet}$ (Kukui et al., 2003; Scaduto, 1995); the presence of MSA in the observed samples and its correlation with other measured organic acids ($r^2 \geq 0.7$ for all low molecular mass organic acids, $r^2 = 0.88$ with oxalate) additionally supports the occurrence of AAOP upwind of fog water collection.

3.6 Mass spectral analysis

Polar organic components of the fog water with $\geq C_4$ were tentatively identified using HPLC-(-)-ESI-HR-ToF-MS. These compounds were biogenic and anthropogenic in origin, including pinic acid and monoterpene-derived organosulfates, and phthalic acid (Table 2). Dicarboxylic and hydroxy-dicarboxylic acids are a prominent group of compounds identified within the polar organic matter of the BYI fog samples. A van Krevelen diagram (Chen et al., 2015; Heald et al., 2010; Mazzoleni et al., 2010; Noziere

ACPD
15, 24871–24908, 2015

et al., 2015) was used to illustrate the distribution of identified organic species (CHO, CHNO, CHOS, CHNOS; Fig. 6) and to distinguish series of compounds differing by functional groups: carbonyl (−2H, +1O; slope = −2); carboxylic acid (−2H, +2O; slope = −1); methyl/methylene (also slope = −1); alcohol (or oxidation of an aldehyde to a carboxylic acid group; slope = 0); or water (slope = +2). In BYI fog samples, series of: (1) saturated di-acids (C_5 through C_7; slope = −0.5), (2) hydroxy-di-acids (C_5–C_7; slope = −0.7), (3) hydroxy-mono-unsaturated di-acids (C_7–C_9; slope = −0.8), (4) mono-unsaturated di-acids (C_4 through C_9; slope = −1), (5) phthalate derivatives with differing oxygen contents (slope = 0); and (6) nitrophenols (slope = −1) are visible in the van Krevelen diagram (Fig. 6). Mean O : C and H : C of ambient aerosol samples (mass-normalized, from aerosol mass spectrometry; Heald et al., 2010; Ng et al., 2011; Chen et al., 2015) typically fall on a line within van Krevelen space at a slope of −1 and *y* intercept of 2 for samples with fresh emissions and a slope of −0.5 for rural/remote samples. Within the molecular level analysis employed here, the slopes between −1 and −0.5 appear to correspond to homologous series of compounds differing by a methylene or methyl group, with differing levels of unsaturation and/or number of hydroxyl groups. The space within the van Krevelen diagram occupied by these identified series indicates they are chemically similar to aged aerosol from previous studies (Chen et al., 2015) and may be analogous to ring-opened and oxygenated species present within the fragmentation scheme of the atmospheric aging process (Kroll et al., 2009).

3.7 Nitrophenols

Four identified nitrophenol species were quantified via HPLC-(-)-ESI-HR-ToF-MS (Table SI-4): 4-nitrophenol (36.4 ± 1.8 nM; max 297 nM), 2-methyl-4-nitrophenol (3.8 ± 0.5 nM; max 42.7 nM), 2,4-dinitrophenol (20.7 ± 0.1 nM; max 74.8 nM), and 2-methyl-4,6-dinitrophenol (0.7 ± 0.1 nM; max 5.1 nM). Concentrations detected in most previous fog and cloud water field studies were ∼ 1–300 nM (Harrison et al., 2005), in the same range as identified in this study. However, the concentrations of 4-nitrophenol measured within cloud water from Mount Tai were as high as 15 µM (Desyaterik et al.,

ACPD
15, 24871–24908, 2015

2013). The lower concentrations measured at BYI vs. at Mount Tai likely reflect the strong influence of aged biomass burning emissions in the Mount Tai region, and may also be a result of aqueous aging in the samples collected at BYI, since species such as 4-nitrophenol are oxidized by $^{\bullet}OH$ in the aqueous phase (Zhang et al., 2003). Other nitrate-containing species (tentatively identified; Table 2) included a second methyl-nitrophenol isomer (m/z^- 152.04, $C_7H_7NO_3$), a hydroxy-nitrophenol (m/z^- 154.02, $C_6H_5NO_4$), a dimethyl-nitrophenol (m/z^- 166.05, $C_8H_9NO_3$), and three other oxygenated nitrophenols (m/z^- 228.02, $C_8H_7NO_7$; m/z^- 284.05, $C_{11}H_{11}NO_8$; and m/z^- 361.16, $C_{15}H_{26}N_2O_8$). These nitrogen-containing organic species may have originated from biomass burning and/or forest fires in Southeast Asia and Eastern Russia during the fog study period. For the three days with quantified fog nitrophenol concentrations above detection limits, large-scale fires were detected in upwind source regions (MODIS data). Levoglucosan concentrations confirmed that the fog on these three days (as well as two other days) was impacted by biomass burning emissions. Concentrations of the biomass burning marker K^+ were additionally above the study mean during those three days and a correlation of $r^2 = 0.93$ ($N = 11$) was observed between nss-K^+ and total quantified nitrophenols as air equivalent concentrations (nmol m^{-3}).

3.8 Organosulfates

Ten organic sulfur (CHOS) species were identified within BYI fog samples (Table 2), eight of which have also been found within rainwater (samples collected in urban and rural New Jersey; Altieri et al., 2009). Most organosulfates identified were likely from oxidation and sulfonation of biogenic emissions, including m/z^- 225.01, 253.04, and 267.06 corresponding to $C_6H_{10}O_7S$, $C_8H_{34}O_7S$ and $C_9H_{16}O_7S$; however, no isoprene-derived organosulfates were detected in the BYI samples (Surratt et al., 2008). Nguyen and coworkers (2014a) observed a compound with the formula $C_8H_{14}O_7S$ in aerosol samples, and Surratt and coworkers (2008) showed that the source may have been esterification of a *d*-limonene oxidation product with sulfate. An observed compound at m/z^- 239.02 with a formula of $C_7H_{12}O_7S$ was previously identified by

ACPD
15, 24871–24908, 2015

Praplan et al. (2014) as an oxidation product of the anthropogenic species 1,3,5-trimethylbenzene. Several pairs of organosulfates appear to have originated from loss of a hydroxyl group: for example, m/z^- 195.03 and 211.03, corresponding to $C_6H_{12}O_5S$ and $C_6H_{12}O_6S$; the latter species was noted to possibly be formed from the sulfonation of a fatty acid (Surratt et al., 2008). CHONS species were also found in the fog samples from BYI, two of which were identified previously as monoterpene oxidation products (Surratt et al., 2008): m/z^- 294.07 with formula $C_{10}H_{17}NO_7S$ and m/z^- 310.06 with formula $C_{10}H_{17}NO_8S$. A compound with the formula $C_{10}H_{17}NO_7S$ was also identified with Fresno fog samples (Mazzoleni et al., 2010). Several CHO species were additionally identified as both biogenic and anthropogenic secondary organic species; for example, 3-methyl-1,2,3-butanetricarboxylic acid (MBTCA) was tentatively identified (m/z^- 189.08 and formula $C_8H_{14}O_5$), as was diaterpenylic acid (m/z^- 189.078; $C_8H_{14}O_5$), which are gas-phase oxidation products of α–pinene (Szmigielski et al., 2007a; Yasmeen et al., 2010).

3.9 Atmospheric aqueous organic processing

Many features of the fog water at BYI, including the organic composition and the humid conditions encountered prior to arrival at the collection site, suggest that components in the fog were highly oxidized. The oxidation may have occurred in the fogs themselves or during upwind transport of wet aerosol later scavenged by the fog. The RH of fog-producing air masses arriving at BYI was high, with only a few time periods at $< 50\,\%$, and mean 65–91 % (Fig. SI-3). Only the air mass intercepted during the fog event on 30 June did not encounter RH $> 80\,\%$ within 72 h of fog formation at BYI. Mixtures of organic and inorganic components including products of aqueous atmospheric aging can easily take up water (growth factors = 1.71 at $\sim 85\,\%$ RH for several organic acids; Wise et al., 2003 and ≤ 1.16 at 85 % RH for chamber-generated secondary organic aerosol; Varutbangkul et al., 2006). It is therefore likely that the aerosol LWC was sufficient to allow radical or even non-radical reactions to occur upwind of the BYI fog collection site (Lim et al., 2010, 2013). The high abundance and large diversity of

ACPD
15, 24871–24908, 2015

organic acids, oxidized sulfur, lack of peroxides, and organosulfates identified within fog samples also support the hypothesis that AAOP reactions took place within wetted aerosol particles, in-cloud/fog during transit of the intercepted air masses to BYI, or within the fog at BYI (Lim et al., 2005; McNeill, 2015).

3.10 Size and microphysical considerations

Changes in LWC, species concentrations, and enrichments of species within large or small droplets can be indicative of many simultaneous microphysical processes: coalescence or condensational growth, evaporation, deposition, and collisions between droplets and interstitial particles (Degefie et al., 2015; Fahey et al., 2005; Seinfeld and Pandis, 2006). Figure 7 shows differences in large and small droplet concentrations of abundant chemical constituents in the BYI fog samples collected on the two stages of the sf-CASCC. Much higher volumes of liquid water were typically collected into the large droplet fraction (> 16 µm) than the small droplet fraction (4–16 µm) at BYI; on average the small fraction comprised only 10 % of the total liquid water volume, indicating relatively large fog droplets made up most of the LWC. All species shown are enriched in the small droplet (4–16 µm) size fraction, with the exception of peroxides; similar observations have previously been reported in many clouds and fogs, especially for species typically associated with submicron aerosol, including sulfate, nitrate, ammonium, and OC (Bator and Collett, 1997; Herckes et al., 2007; Munger et al., 1989). As in most of these prior observations, the pH in large BYI fog droplets was also typically higher than in small droplets. Differences in pH among cloud drops can give rise to differences in the rates of pH-dependent chemical reaction rates, including the aqueous oxidation of S(IV) to sulfate by ozone or by oxygen in the presence of trace metal catalysts (Collett et al., 1994; Hegg and Larson, 1990; Rao and Collett, 1998). Enrichment of solutes in large or small fog drops can also affect rates of removal by fog drop deposition (e.g., Fahey et al., 2005; Herckes et al., 2007; Hoag et al., 1999).

ACPD
15, 24871–24908, 2015

4 Conclusions

The fogs at BYI were on average slightly acidic and the chemical composition was dominated by NH_4NO_3 from long-range transport, with contributions from anthropogenic nss-SO_4^{-2}, marine NaCl, and a variety of organic compounds. Biomass burning activities throughout Eastern Russia and Southeast Asia appear to have contributed K^+ and organic species, including nitrophenols, in some periods. Organosulfate species deriving from oxidation products of monoterpenes (e.g., Surratt et al., 2008; Nguyen et al., 2014) were observed, several of which have been identified in aqueous atmospheric samples in the past (Altieri et al., 2009; Mazzoleni et al., 2010). Low concentrations of S(IV), high concentrations of SO_4^{-2}, and generally low concentrations of peroxides suggest that chemical components of the fog water were highly oxidized during upwind transport and/or within the local fog. Low molecular mass organic acids such as acetate, formate, and succinate accounted for 36–69 % of TOC, a typically higher fraction than observed in fogs from other environments, with acetate, formate, succinate, oxalate, and maleate each contributing > 5 % of TOC on average. Further analysis of the fog organic matter via HPLC-(-)-ESI-HR-ToF-MS revealed homologous series of dicarboxylic acids and nitrophenols. The position within van Krevelen space occupied by identified organics matches well with the fragmentation aging regime (at high oxidation state) shown by Kroll and coworkers (2009).

Future studies of fog or cloud water composition in the region should include the characterization of carbonyl species which have been cited as some of the most important AAOP reactants (Ervens et al., 2011) and are direct oxidation precursors of organic acids. Additional studies to analyze the evolution of gaseous, particulate, and aqueous phase organics during fog events as well as the advancement of laboratory simulated reactions will be essential in more fully characterizing AAOP reactions and aqSOA formation.

ACPD
15, 24871–24908, 2015

Data availability

Processed data are available in the Supplement to this article. Raw data are archived at the Colorado State University Atmospheric Science Department and are available on request.

The Supplement related to this article is available online at doi:10.5194/acpd-15-24871-2015-supplement.

Acknowledgements. The authors gratefully acknowledge the work of Sungwon Cho and Jungmin Yeom during the field campaign at BYI. This work was made possible through funding provided by a National Science Foundation (NSF) East Asia and Pacific Summer Institutes (EAPSI) Fellowship (1414725), which was funded in part by the National Research Foundation (NRF) of Korea (NRF2014R1A1A1007947). Research funding was also provided by NSF grant AGS-1050052; purchase of the HPLC-(-)-ESI-HR-ToF-MS system was supported through an NSF MRI grant (ATM-0521643). The authors gratefully acknowledge the employees of the Korean NIER at BYI, the laboratory of John Dominick Fisk in the Chemistry Department at CSU for use of the Labteq fluorescence plate reader, Hermann Gerber for assistance with the PVM-100, and the NOAA Air Resources Laboratory (ARL) for the provision of the HySPLIT transport and dispersion model (http://www.ready.noaa.gov) used in this publication.

References

Aiken, A. C., Decarlo, P. F., Kroll, J. H., Worsnop, D. R., Huffman, J. A., Docherty, K. S., Ulbrich, I. M., Mohr, C., Kimmel, J. R., Super, D., Sun, Y., Zhang, Q., Trimborn, A., Northway, M., Zieman, P. J., Canagaratna, M. R., Onasch, T. B., Alfarra, M. R., Prevot, A. S. H., Dommen, J., Duplissy, J., Metzger, A., Baltensperger, U., and Jimenez, J. L.: O/C and OM/OC Ratios of Primary, Secondary, and Ambient Organic Aerosols with High-Resolution Time-of-Flight Aerosol Mass Spectrometry, Environ. Sci. Technol., 42, 4478–4485, doi:10.1021/es703009q, 2008.

Altieri, K. E., Turpin, B. J., and Seitzinger, S. P.: Oligomers, organosulfates, and nitrooxy organosulfates in rainwater identified by ultra-high resolution electrospray ionization FT-ICR mass spectrometry, Atmos. Chem. Phys., 9, 2533–2542, doi:10.5194/acp-9-2533-2009, 2009.

Andreae, M. O.: Soot carbon and excess fine potassium: Long-range transport of combustion-derived aerosols, Science, 220, 1148–1151, doi:10.1126/science.220.4602.1148, 1983.

Bator, A. and Collett, J. L.: Cloud chemistry varies with drop size, J. Geophys. Res., 102, 28071–28078, doi:10.1029/97JD02306, 1997.

Benedict, K. B., Lee, T., and Collett, J. L.: Cloud water composition over the southeastern Pacific Ocean during the VOCALS regional experiment, Atmos. Environ., 46, 104–114, doi:10.1016/j.atmosenv.2011.10.029, 2012.

Bian, Q., Huang, X. H. H., and Yu, J. Z.: One-year observations of size distribution characteristics of major aerosol constituents at a coastal receptor site in Hong Kong – Part 1: Inorganic ions and oxalate, Atmos. Chem. Phys., 14, 9013–9027, doi:10.5194/acp-14-9013-2014, 2014.

Boris, A. J., Desyaterik, Y., and Collett, J. L.: How do components of real cloud water affect aqueous pyruvate oxidation?, Atmos. Res., 143, 95–106, doi:10.1016/j.atmosres.2014.02.004, 2014.

Borrás, E. and Tortajada-Genaro, L. A.: Secondary organic aerosol formation from the photo-oxidation of benzene, Atmos. Environ., 47, 154–163, doi:10.1016/j.atmosenv.2011.11.020, 2012.

Brinkmann, T., Hörsch, P., Sartorius, D., and Frimmel, F. H.: Photoformation of low-molecular-weight organic acids from brown water dissolved organic matter, Environ. Sci. Technol., 37, 4190–4198, doi:10.1021/es0263339, 2003.

Chen, Q., Heald, C. L., Jimenez, J. L., Canagaratna, M. R., He, L., Huang, X., Campuzano-jost, P., Palm, B. B., Poulain, L., Kuwata, M., Martin, S. T., Abbatt, J. P. D., Lee, A. K. Y., and Liggio, J.: Elemental composition of organic aerosol: the gap between ambient and laboratory measurements, Geophys. Res. Lett., 42, 1–8, doi:10.1002/2015GL063693, 2015.

Cho, Y., Kim, M., and Kim, B.: Sea fog around the Korean Peninsula, J. Appl. Meteorol., 39, 2473–2479, doi:10.1175/1520-0450(2000)039<2473:SFATKP>2.0.CO;2, 2000.

Claeys, M., Iinuma, Y., Szmigielski, R., Surratt, J. D., Blockhuys, F., Van Alsenoy, C., Böge, O., Sierau, B., Gómez-González, Y., Vermeylen, R., Van der Veken, P., Shahgholi, M., Chan, A. W. H., Herrmann, H., Seinfeld, J. H., and Maenhaut, W.: Terpenylic acid and related

ACPD
15, 24871–24908, 2015

compounds from the oxidation of alpha-pinene: implications for new particle formation and growth above forests., Environ. Sci. Technol., 43, 6976–82, doi:10.1021/es9007596, 2009.
Collett, J. L., Bator, A., Rao, X., and Demoz, B. B.: Acidity variations across the cloud drop size spectrum and their influence on rates of atmospheric sulfate production, Geophys. Res. Lett., 21, 2393–2396, doi:10.1029/94GL02480, 1994.
Collett, J. L., Bator, A., Sherman, D. E., Moore, K. F., Hoag, K. J., Demoz, B. B., Rao, X., and Reilly, J. E.: The chemical composition of fogs and intercepted clouds in the United States, Atmos. Res., 64, 29–40, doi:10.1016/S0169-8095(02)00077-7, 2002.
Collett, J. L., Herckes, P., Youngster, S., and Lee, T.: Processing of atmospheric organic matter by California radiation fogs, Atmos. Res., 87, 232–241, doi:10.1016/j.atmosres.2007.11.005, 2008.
Daumit, K. E., Carrasquillo, A. J., Hunter, J. F., and Kroll, J. H.: Laboratory studies of the aqueous-phase oxidation of polyols: submicron particles vs. bulk aqueous solution, Atmos. Chem. Phys., 14, 10773–10784, doi:10.5194/acp-14-10773-2014, 2014.
Decesari, S., Facchini, M., Fuzzi, S., Mcfiggans, G., Coe, H., and Bower, K.: The water-soluble organic component of size-segregated aerosol, cloud water and wet depositions from Jeju Island during ACE-Asia, Atmos. Environ., 39, 211–222, doi:10.1016/j.atmosenv.2004.09.049, 2005.
Degefie, D. T., El-Madany, T.-S., Hejkal, J., Held, M., Dupont, J.-C., Haeffelin, M., and Klemm, O.: Microphysics and energy and water fluxes of various fog types at SIRTA, France, Atmos. Res., 151, 162–175, doi:10.1016/j.atmosres.2014.03.016, 2015.
Demoz, B. B., Collett, J. L., and Daube, B. C.: On the caltech active strand cloudwater collectors, Atmos. Res., 41, 47–62, doi:10.1016/0169-8095(95)00044-5, 1996.
Desyaterik, Y., Sun, Y., Shen, X., Lee, T., Wang, X., Wang, T., and Collett, J. L.: Speciation of "brown" carbon in cloud water impacted by agricultural biomass burning in eastern China, J. Geophys. Res. Atmos., 118, 7389–7399, doi:10.1002/jgrd.50561, 2013.
Edney, E. O., Driscoll, D. J., Speer, R. E., Weathers, W. S., Kleindienst, T. E., Li, W., and Smith, D. F.: Impact of aerosol liquid water on secondary organic aerosol yields of irradiated toluene/propylene/NO_x/$(NH_4)_2SO_4$/air mixtures, Atmos. Environ., 34, 3907–3919, 2000.
Ervens, B., Herckes, P., Feingold, G., Lee, T., Collett, J. L., and Kreidenweis, S. M.: On the drop-size dependence of organic acid and formaldehyde concentrations in fog, J. Atmos. Chem., 46, 239–269, doi:10.1023/A:1026393805907, 2003.

ACPD
15, 24871–24908, 2015

Ervens, B., Turpin, B. J., and Weber, R. J.: Secondary organic aerosol formation in cloud droplets and aqueous particles (aqSOA): a review of laboratory, field and model studies, Atmos. Chem. Phys., 11, 11069–11102, doi:10.5194/acp-11-11069-2011, 2011.

Ervens, B., Sorooshian, A., Lim, Y. B., and Turpin, B. J.: Key parameters controlling OH-initiated formation of secondary organic aerosol in the aqueous phase (asSOA), J. Geophys. Res.-Atmos., 119, 3997–4016, doi:10.1002/2013JD021021, 2014.

Fahey, K. M., Pandis, S. N., Collett, J. L., and Herckes, P.: The influence of size-dependent droplet composition on pollutant processing by fogs, Atmos. Environ., 39, 4561–4574, doi:10.1016/j.atmosenv.2005.04.006, 2005.

Fu, T.-M., Jacob, D. J., Wittrock, F., Burrows, J. P., Vrekoussis, M., and Henze, D. K.: Global budgets of atmospheric glyoxal and methylglyoxal, and implications for formation of secondary organic aerosols, J. Geophys. Res., 113, D15303, doi:10.1029/2007JD009505, 2008.

Fuzzi, S., Facchini, M. C., Orsi, G., Lind, J. A., Wobrock, W., Kessell, M., Maser, R., Jaeschke, W., Enderle, K. H., Arends, B. G., Berner, A., Solly, I., Kruisz, C., Reischl, G., Pahl, S., Kaminski, U., Winkler, P., Ogren, J. A., Noone, K. J., Hallberg, A., Fierlinger-Oberlinninger, H., Puxbaum, H., Marzorati, A., Hansson, H.-C., Wiedensohler, A., Svenningsson, I. B., Martinsson, B. G., Schell, D., and Georgii, H. W.: The Po Valley Fog Experiment 1989: an overview, Tellus B, 44, 448–468, doi:10.1034/j.1600-0889.1992.t01-4-00002.x, 1992.

Gerber, H.: Direct measurement of suspended particulate volume concentration and far-infrared extinction coefficient with a laser-diffraction instrument, Appl. Optics, 30, 4824–4831, doi:10.1364/AO.30.004824, 1991.

Harrison, M., Barra, S., Borghesi, D., Vione, D., Arsene, C., and Iulianolariu, R.: Nitrated phenols in the atmosphere: a review, Atmos. Environ., 39, 231–248, doi:10.1016/j.atmosenv.2004.09.044, 2005.

Heald, C. L., Jacob, D. J., Park, R. J., Russell, L. M., Huebert, B. J., Seinfeld, J. H., Liao, H., and Weber, R. J.: A large organic aerosol source in the free troposphere missing from current models, Geophys. Res. Lett., 32, 2–5, doi:10.1029/2005GL023831, 2005.

Heald, C. L., Kroll, J. H., Jimenez, J. L., Docherty, K. S., DeCarlo, P. F., Aiken, A. C., Chen, Q., Martin, S. T., and Farmer, D. K.: A simplified description of the evolution of organic aerosol composition in the atmosphere, Geophys. Res. Lett., 37, L08803, doi:10.1029/2010GL042737, 2010.

ACPD
15, 24871–24908, 2015

Hegg, D. A. and Larson, T. V.: The effects of microphysical parameterization on model predictions of sulfate production in clouds, Tellus B, 42, 272–284, 1990.
Herckes, P., Hannigan, M. P., Trenary, L., Lee, T., and Collett, J. L.: Organic compounds in radiation fogs in Davis (California), Atmos. Res., 64, 99–108, doi:10.1016/S0169-8095(02)00083-2, 2002.
Herckes, P., Chang, H., Lee, T., and Collett, J. L.: Air pollution processing by radiation fogs, Water Air Soil Pollut., 181, 65–75, doi:10.1007/s11270-006-9276-x, 2007.
Herckes, P., Valsaraj, K. T., and Collett, J. L.: A review of observations of organic matter in fogs and clouds: origin, processing and fate, Atmos. Res., 132–133, 434–449, doi:10.1016/j.atmosres.2013.06.005, 2013.
Hoag, K. J., Collett, J. L., and Pandis, S. N.: The influence of drop size-dependent fog chemistry on aerosol processing by San Joaquin Valley fogs, Atmos. Environ., 33, 4817–4832, doi:10.1016/S1352-2310(99)00268-X, 1999.
Kahnt, A., Behrouzi, S., Vermeylen, R., Safi Shalamzari, M., Vercauteren, J., Roekens, E., Claeys, M., and Maenhaut, W.: One-year study of nitro-organic compounds and their relation to wood burning in PM_{10} aerosol from a rural site in Belgium, Atmos. Environ., 81, 561–568, doi:10.1016/j.atmosenv.2013.09.041, 2013.
Kalberer, M., Yu, J., Cocker, D. R., Flagan, R. C., and Seinfeld, J. H.: Aerosol formation in the cyclohexene–ozone system, Environ. Sci. Technol., 34, 4894–4901, doi:10.1021/es001180f, 2000.
Kamens, R. M., Zhang, H., Chen, E. H., Zhou, Y., Parikh, H. M., Wilson, R. L., Galloway, K. E., and Rosen, E. P.: Secondary organic aerosol formation from toluene in an atmospheric hydrocarbon mixture: water and particle seed effects, Atmos. Environ., 45, 2324–2334, doi:10.1016/j.atmosenv.2010.11.007, 2011.
Kawamura, K. and Ikushima, K.: Seasonal changes in the distribution of dicarboxylic acids in the urban atmosphere, Environ. Sci. Technol., 27, 2227–2235, doi:10.1021/es00047a033, 1993.
Kawamura, K. and Kaplan, I.: Motor exhaust emissions as a primary source for dicarboxylic acids in Los Angeles ambient air, Environ. Sci. Technol., 21, 105–110, doi:10.1021/es00155a014, 1987.
Kim, M.-G., Lee, B.-K., and Kim, H.-J.: Cloud/fog water chemistry at a high elevation site in South Korea, J. Atmos. Chem., 55, 13–29, doi:10.1007/s10874-005-9004-8, 2006.

ACPD
15, 24871–24908, 2015

Kleindienst, T. E., Smith, D. F., Li, W., Edney, E. O., Driscoll, D. J., Speer, R. E., and Weathers, W. S.: Secondary organic aerosol formation from the oxidation of aromatic hydrocarbons in the presence of dry submicron ammonium sulfate aerosol, Atmos. Environ., 33, 3669–3681, doi:10.1016/S1352-2310(99)00121-1, 1999.

Kroll, J. H., Smith, J. D., Dung, L. C., Kessler, S. H., Worsnop, D. R., and Wilson, K. R.: Measurement of fragmentation and functionalization pathways in the heterogeneous oxidation of oxidized organic aerosol, Phys. Chem. Chem. Phys., 11, 8005–8014, doi:10.1039/b916865f, 2009.

Kukui, A., Borissenko, D., Laverdet, G., and Le Bras, G.: Gas-phase reactions of OH radicals with dimethyl sulfoxide and methane sulfinic acid using turbulent flow reactor and chemical ionization mass spectrometry, J. Phys. Chem. A, 107, 5732–5742, doi:10.1021/jp0276911, 2003.

Lee, T.: Characterizing Ionic Components of Aerosol in Rural Environments: Temporal Variability, Size Distributions, and the Form of Particle Nitrate, thesis, Department of Atmospheric Science, Colorado State University in Fort Collins, Colorado, USA, 2007.

Lee, T., Sullivan, A. P., Mack, L., Jimenez, J. L., Kreidenweis, S. M., Onasch, T. B., Worsnop, D. R., Malm, W., Wold, C. E., Hao, W. M., and Collett, J. L.: Chemical smoke marker emissions during flaming and smoldering phases of laboratory open burning of wildland fuels, Aerosol Sci. Tech., 44, I–V, doi:10.1080/02786826.2010.499884, 2010.

Lee, T., Lee, G., Choi, J., Ahn, J. Y., Park, J. S., Atwood, S. A., Schurman, M., Chung, Y., and Collett, J. L.: Characterization of aerosol composition, concentrations, and sources at Baeong–Yeong Island, Korea using an aerosol mass spectrometer, Atmos. Environ., accepted, 2015.

Lelieveld, J. and Crutzen, P.: The role of clouds in tropospheric photochemistry, J. Atmos. Chem., 12, 229–267, doi:10.1007/BF00048075, 1991.

Li, P., Li, X., Yang, C., Wang, X., Chen, J., and Collett, J. L.: Fog water chemistry in Shanghai, Atmos. Environ., 45, 4034–4041, doi:10.1016/j.atmosenv.2011.04.036, 2011.

Lim, H., Carlton, A. G., and Turpin, B. J.: Isoprene forms secondary organic aerosol through cloud processing: model simulations, Environ. Sci. Technol., 39, 4441–4446, doi:10.1021/es048039h, 2005.

Lim, Y. B., Tan, Y., Perri, M. J., Seitzinger, S. P., and Turpin, B. J.: Aqueous chemistry and its role in secondary organic aerosol (SOA) formation, Atmos. Chem. Phys., 10, 10521–10539, doi:10.5194/acp-10-10521-2010, 2010.

ACPD
15, 24871–24908, 2015

Lim, Y. B., Tan, Y., and Turpin, B. J.: Chemical insights, explicit chemistry, and yields of secondary organic aerosol from OH radical oxidation of methylglyoxal and glyoxal in the aqueous phase, Atmos. Chem. Phys., 13, 8651–8667, doi:10.5194/acp-13-8651-2013, 2013.

Lin, G., Sillman, S., Penner, J. E., and Ito, A.: Global modeling of SOA: the use of different mechanisms for aqueous-phase formation, Atmos. Chem. Phys., 14, 5451–5475, doi:10.5194/acp-14-5451-2014, 2014.

Liu, J., Horowitz, L., and Fan, S.: Global in-cloud production of secondary organic aerosols: Implementation of a detailed chemical mechanism in the GFDL atmospheric model AM3, J. Geophys. Res.-Atmos., 117, 1–15, doi:10.1029/2012JD017838, 2012.

Mazzoleni, L. R., Ehrmann, B. M., Shen, X., Marshall, A. G., and Collett, J. L.: Water-soluble atmospheric organic matter in fog: exact masses and chemical formula identification by ultrahigh-resolution fourier transform ion cyclotron resonance mass spectrometry, Environ. Sci. Technol., 44, 3690–3697, doi:10.1021/es903409k, 2010.

McCulloch, A., Aucott, M. L., Benkovitz, C. M., Graedel, T. E., Kleiman, G., Midgley, P. M., and Li, Y.-F.: Global emissions of hydrogen chloride and chloromethane from coal combustion, incineration and industrial activities: reactive chlorine emissions inventory, J. Geophys. Res., 104, 8391–8403, doi:10.1029/1999JD900025, 1999.

McNeill, V. F.: Aqueous organic chemistry in the atmosphere: sources and chemical processing of organic aerosols, Environ. Sci. Technol., 49, 1237–1244, doi:10.1021/es5043707, 2015.

Moore, K. F., Sherman, D. E., Reilly, J. E., and Collett, J. L.: Drop size-dependent chemical composition in clouds and fogs. Part I. Observations, Atmos. Environ., 38, 1389–1402, doi:10.1016/j.atmosenv.2003.12.013, 2004a.

Moore, K. F., Sherman, D. E., Reilly, J. E., Hannigan, M. P., Lee, T., and Collett, J. L.: Drop size-dependent chemical composition of clouds and fogs. Part II: Relevance to interpreting the aerosol/trace gas/fog system, Atmos. Environ., 38, 1403–1415, doi:10.1016/j.atmosenv.2003.12.014, 2004b.

Mouri, H. and Okada, K.: Shattering and modification of sea-salt particles in the marine atmosphere, Geophys. Res. Lett., 20, 49–52, doi:10.2467/mripapers.57.47, 1993.

Munger, J., Collett, J., Daube, B., and Hoffmann, M.: Carboxylic acids and carbonyl compounds in southern California clouds and fogs, Tellus B, 41, 230–242, doi:10.1111/j.1600-0889.1989.tb00303.x, 1989.

ACPD
15, 24871–24908, 2015

Narukawa, M. and Kawamura, K.: Distribution of dicarboxylic acids and carbon isotopic compositions in aerosols from 1997 Indonesian forest fires, Geophys. Res. Lett., 26, 3101–3104, doi:10.1029/1999GL010810, 1999.

Ng, N. L., Canagaratna, M. R., Jimenez, J. L., Chhabra, P. S., Seinfeld, J. H., and Worsnop, D. R.: Changes in organic aerosol composition with aging inferred from aerosol mass spectra, Atmos. Chem. Phys., 11, 6465–6474, doi:10.5194/acp-11-6465-2011, 2011.

Nguyen, Q. T., Christensen, M. K., Cozzi, F., Zare, A., Hansen, A. M. K., Kristensen, K., Tulinius, T. E., Madsen, H. H., Christensen, J. H., Brandt, J., Massling, A., Nøjgaard, J. K., and Glasius, M.: Understanding the anthropogenic influence on formation of biogenic secondary organic aerosols in Denmark via analysis of organosulfates and related oxidation products, Atmos. Chem. Phys., 14, 8961–8981, doi:10.5194/acp-14-8961-2014, 2014.

Nguyen, T. B., Roach, P. J., Laskin, J., Laskin, A., and Nizkorodov, S. A.: Effect of humidity on the composition of isoprene photooxidation secondary organic aerosol, Atmos. Chem. Phys., 11, 6931–6944, doi:10.5194/acp-11-6931-2011, 2011.

Nguyen, T. K. V., Petters, M. D., Suda, S. R., Guo, H., Weber, R. J., and Carlton, A. G.: Trends in particle-phase liquid water during the Southern Oxidant and Aerosol Study, Atmos. Chem. Phys., 14, 10911–10930, doi:10.5194/acp-14-10911-2014, 2014.

Noziere, B., Kalberer, M., Claeys, M., Allan, J., Anna, B. D., Decesari, S., Finessi, E., Glasius, M., Grgic, I., Hamilton, J. F., Ho, T., Iinuma, Y., Jaoui, M., Kahnt, A., Kampf, C. J., Kourtchev, I., Maenhaut, W., Marsden, N., Saarikoski, S., Schnelle-kreis, J., Surratt, J. D., Szidat, S., Szmigielski, R., and Wisthaler, A.: The molecular identification of organic compounds in the atmosphere: state of the art and challenges, Chem. Rev., 115, 3919–3983, doi:10.1021/cr5003485, 2015.

Pandis, S. N., Seinfeld, J. H., and Pilinis, C.: The smog-fog-smog cycle and acid deposition, J. Geophys. Res., 95, 18489–18500, doi:10.1029/JD095iD11p18489, 1990.

Praplan, A. P., Hegyi-Gaeggeler, K., Barmet, P., Pfaffenberger, L., Dommen, J., and Baltensperger, U.: Online measurements of water-soluble organic acids in the gas and aerosol phase from the photooxidation of 1,3,5-trimethylbenzene, Atmos. Chem. Phys., 14, 8665–8677, doi:10.5194/acp-14-8665-2014, 2014.

Radojevic, M. and Bashkin, V. N.: Practical Environmental Analysis, The Royal Society of Chemistry, Cambridge, UK, 2006.

Raja, S., Raghunathan, R., Yu, X.-Y., Lee, T., Chen, J., Kommalapati, R. R., Murugesan, K., Shen, X., Qingzhong, Y., Valsaraj, K. T., and Collett, J. L.: Fog chem-

ACPD
15, 24871–24908, 2015

istry in the Texas–Louisiana Gulf Coast corridor, Atmos. Environ., 42, 2048–2061, doi:10.1016/j.atmosenv.2007.12.004, 2008.
Rao, X. and Collett, J. L.: Behavior of S(IV) and formaldehyde in a chemically heterogeneous cloud, Environ. Sci. Technol., 29, 1023–1031, doi:10.1021/es00004a024, 1995.
Rao, X. and Collett, J. L.: The Drop Size-Dependence of Iron and Manganese Concentrations in Clouds and Fogs: Implications for Sulfate Production, J. Atmos. Chem., 30, 273–289, 1998.
Reilly, J. E., Rattigan, O. V, Moore, K. F., Judd, C., Eli Sherman, D., Dutkiewicz, V. A., Kreidenweis, S. M., Husain, L., and Collett, J. L.: Drop size-dependent S(IV) oxidation in chemically heterogeneous radiation fogs, Atmos. Environ., 35, 5717–5728, doi:10.1016/S1352-2310(01)00373-9, 2001.
Sareen, N., Schwier, A. N., Shapiro, E. L., Mitroo, D., and McNeill, V. F.: Secondary organic material formed by methylglyoxal in aqueous aerosol mimics, Atmos. Chem. Phys., 10, 997–1016, doi:10.5194/acp-10-997-2010, 2010.
Scaduto, R. C. J.: Oxidation of DMSO and methanesulfinic acid by the hydroxyl radical, Free Radical Bio. Med., 18, 271–277, doi:10.1016/0891-5849(94)E0139-A, 1995.
Seinfeld, J. H. and Pandis, S. N.: Atmospheric Chemistry and Physics: from Air Pollution to Climate Change, John Wiley & Sons, Inc., Hoboken, New Jersey, 2006.
Shen, X.: Aqueous Phase Sulfate Production in Clouds at Mt. Tai in Eastern China, thesis, Department of Atmospheric Science, Colorado State University in Fort Collins, Colorado, USA, 2011.
Shen, X., Lee, T., Guo, J., Wang, X., Li, P., Xu, P., Wang, Y., Ren, Y., Wang, W., Wang, T., Li, Y., Carn, S. A., and Collett, J. L.: Aqueous phase sulfate production in clouds in eastern China, Atmos. Environ., 62, 502–511, doi:10.1016/j.atmosenv.2012.07.079, 2012.
Sorooshian, A. and Varutbangkul, V.: Oxalic acid in clear and cloudy atmospheres: analysis of data from International Consortium for Atmospheric Research on Transport and Transformation 2004, J. Geophys. Res., 111, 1–10, doi:10.1029/2005JD006880, 2006.
Straub, D. J., Lee, T., and Collett, J. L.: Chemical composition of marine stratocumulus clouds over the eastern Pacific Ocean, J. Geophys. Res., 112, D04307, doi:10.1029/2006JD007439, 2007.
Sullivan, A. P., Holden, A. S., Patterson, L. A., McMeeking, G. R., Kreidenweis, S. M., Malm, W. C., Hao, W. M., Wold, C. E., and Collett, J. L.: A method for smoke marker measurements and its potential application for determining the contribution of biomass burning

ACPD
15, 24871–24908, 2015

from wildfires and prescribed fires to ambient $PM_{2.5}$ organic carbon, J. Geophys. Res., 113, D22302, doi:10.1029/2008JD010216, 2008.

Surratt, J. D., Gómez-González, Y., Chan, A. W. H., Vermeylen, R., Shahgholi, M., Kleindienst, T. E., Edney, E. O., Offenberg, J. H., Lewandowski, M., Jaoui, M., Maenhaut, W., Claeys, M., Flagan, R. C., and Seinfeld, J. H.: Organosulfate formation in biogenic secondary organic aerosol, J. Phys. Chem. A, 112, 8345–8378, doi:10.1021/jp802310p, 2008.

Szmigielski, R., Surratt, J. D., Gómez-González, Y., van der Veken, P., Kourtchev, I., Vermeylen, R., Blockhuys, F., Jaoui, M., Kleindienst, T. E., Lewandowski, M., Offenberg, J. H., Edney, E. O., Seinfeld, J. H., Maenhaut, W., and Claeys, M.: 3-methyl-1,2,3-butanetricarboxylic acid: an atmospheric tracer for terpene secondary organic aerosol, Geophys. Res. Lett., 34, 2–7, doi:10.1029/2007GL031338, 2007a.

Szmigielski, R., Surratt, J. D., Vermeylen, R., Szmigielska, K., Kroll, J. H., Ng, N. L., Murphy, S. M., Sorooshian, A., Seinfeld, J. H., and Claeys, M.: Characterization of 2-methylglyceric acid oligomers in secondary organic aerosol formed from the photooxidation of isoprene using trimethylsilylation and gas chromatography/ion trap mass spectrometry, J. Mass Spectrom., 42, 101–116, doi:10.1002/jms.1146, 2007b.

Varutbangkul, V., Brechtel, F. J., Bahreini, R., Ng, N. L., Keywood, M. D., Kroll, J. H., Flagan, R. C., Seinfeld, J. H., Lee, A., and Goldstein, A. H.: Hygroscopicity of secondary organic aerosols formed by oxidation of cycloalkenes, monoterpenes, sesquiterpenes, and related compounds, Atmos. Chem. Phys., 6, 2367–2388, doi:10.5194/acp-6-2367-2006, 2006.

Wang, Y., Guo, J., Wang, T., Ding, A., Gao, J., Zhou, Y., Collett, J. L., and Wang, W.: Influence of regional pollution and sandstorms on the chemical composition of cloud/fog at the summit of Mt. Taishan in northern China, Atmos. Res., 99, 434–442, doi:10.1016/j.atmosres.2010.11.010, 2011.

Wise, M. E., Surratt, J. D., Curtis, D. B., Shilling, J. E., and Tolbert, M. A.: Hygroscopic growth of ammonium sulfate/dicarboxylic acids, J. Geophys. Res., 108, 4638–4376, doi:10.1029/2003JD003775, 2003.

Wonaschuetz, A., Sorooshian, A., Ervens, B., Chuang, P. Y., Feingold, G., Murphy, S. M., de Gouw, J., Warneke, C., and Jonsson, H. H.: Aerosol and gas re-distribution by shallow cumulus clouds: An investigation using airborne measurements, J. Geophys. Res., 117, D17202, doi:10.1029/2012JD018089, 2012.

Yamasoe, M., Artaxo, P., Miguel, A., and Allen, A.: Chemical composition of aerosol particles from direct emissions of vegetation fires in the Amazon Basin: water-soluble species

ACPD
15, 24871–24908, 2015

and trace elements, Atmos. Environ., 34, 1641–1653, doi:10.1016/S1352-2310(99)00329-5, 2000.

Yasmeen, F., Vermeylen, R., Szmigielski, R., Iinuma, Y., Böge, O., Herrmann, H., Maenhaut, W., and Claeys, M.: Terpenylic acid and related compounds: precursors for dimers in secondary organic aerosol from the ozonolysis of α- and β-pinene, Atmos. Chem. Phys., 10, 9383–9392, doi:10.5194/acp-10-9383-2010, 2010.

Yu, J. Z., Huang, X.-F., Xu, J., and Hu, M.: When aerosol sulfate goes up, so does oxalate: implication for the formation mechanisms of oxalate., Environ. Sci. Technol., 39, 128–133, doi:10.1021/es049559f, 2005.

Zhang, Q., Worsnop, D. R., Canagaratna, M. R., and Jimenez, J. L.: Hydrocarbon-like and oxygenated organic aerosols in Pittsburgh: insights into sources and processes of organic aerosols, Atmos. Chem. Phys., 5, 3289–3311, doi:10.5194/acp-5-3289-2005, 2005.

Zhang, S.-P., Xie, S.-P., Liu, Q.-Y., Yang, Y.-Q., Wang, X.-G., and Ren, Z.-P.: Seasonal variations of yellow sea fog: observations and mechanisms, J. Climate, 22, 6758–6772, doi:10.1175/2009JCLI2806.1, 2009.

Zhang, W., Xiao, X., An, T., and Song, Z.: Kinetics, degradation pathway and reaction mechanism of advanced oxidation of 4-nitrophenol in water by a UV/H_2O_2 process, J. Chem. Technol. Biot., 794, 788–794, doi:10.1002/jctb.864, 2003.

Zhang, X., Arimoto, R., An, Z., Chen, T., Zhang, G., Zhu, G., and Wang, X.: Atmospheric trace elements over source regions for Chinese dust: concentrations, sources and atmospheric deposition on the Loess plateau, Atmos. Environ. A-Gen., 27, 2051–2067, doi:10.1016/0960-1686(93)90277-6, 1993.

Zheng, M., Salmon, L. G., Schauer, J. J., Zeng, L., Kiang, C. S., Zhang, Y., and Cass, G. R.: Seasonal trends in $PM_{2.5}$ source contributions in Beijing, China, Atmos. Environ., 39, 3967–3976, doi:10.1016/j.atmosenv.2005.03.036, 2005.

Zuo, Y. and Hoigné, J.: Photochemical decomposition of oxalic, glyoxalic and pyruvic acid catalysed by iron in atmospheric waters, Atmos. Environ., 2, 1231–1239, doi:10.1016/1352-2310(94)90270-4, 1994.

ACPD
15, 24871–24908, 2015

Table 1. Mean, minimum, and maximum concentrations of organic and inorganic species quantified in fog samples collected at BYI.

Chemical	Unit	No. Samples	Aqueous concentration Mean	Min	Max	LOD	Uncertainty (95 % CI)	Air equivalent concentration Mean	Unit
pH	–	11	3.94	3.48	5.00	–	–	11.8	$nmol\,m^{-3}$
Peroxides	µM	11	7.8	0.4	58.9	0.2	0.2	0.45	$nmol\,m^{-3}$
S(IV)	µM	11	2.36	0.25	6.27	0.18	0.01	0.12	$nmol\,m^{-3}$
HCHO	µM	10	7	< LOD	21	5	2	0.65	$nmol\,m^{-3}$
TOC	$mg\,C\,L^{-1}$	8	15.3	3.60	24.8	0.26	0.03	480	$ng\,C\,m^{-3}$
Cl^-	µM	14	253	22	900	3	3	9.29	$nmol\,m^{-3}$
NO_2^-	µM	14	2.1	< LOD	5.6	0.9	0.9	0.18	$nmol\,m^{-3}$
NO_3^-	µM	14	1260	185	4900	1	10	49.0	$nmol\,m^{-3}$
SO_4^{-2}	µM	14	730	72.0	2270	7.2	0.4	26.6	$nmol\,m^{-3}$
Na^+	µM	14	551	24	2920	2	2	7.55	$nmol\,m^{-3}$
NH_4^+	µM	14	2220	253	6090	7	4	97.8	$nmol\,m^{-3}$
K^+	µM	14	83	16	172	1	2	3.17	$nmol\,m^{-3}$
Mg^{+2}	µM	14	73	13	276	0.5	1	2.53	$nmol\,m^{-3}$
Ca^{+2}	µM	14	77	12	217	0.2	1	3.23	$nmol\,m^{-3}$
Acetate	µM	11	138	19.3	640	2.36	0.01	4.77	$nmol\,m^{-3}$
Formate	µM	11	120	1.77	532	1.47	0.05	8.47	$nmol\,m^{-3}$
Oxalate	µM	11	41.5	5.86	110	1.47	0.03	1.99	$nmol\,m^{-3}$
Succinate	µM	11	22.9	3.31	52.6	0.74	0.01	1.29	$nmol\,m^{-3}$
Maleate	µM	11	21.1	3.04	58.8	0.29	0.02	0.72	$nmol\,m^{-3}$
Malonate	µM	11	10.7	1.48	24.8	0.45	0.01	0.46	$nmol\,m^{-3}$
Pyruvate	µM	11	9.19	0.79	38.8	0.23	0.02	0.48	$nmol\,m^{-3}$
MSA	µM	11	7.75	1.77	18.6	0.18	0.01	0.30	$nmol\,m^{-3}$
Glutarate	µM	11	6.5	0.92	18.3	0.66	0.02	0.30	$nmol\,m^{-3}$
Valerate	µM	11	1.03	0.21	3.78	0.06	0.01	0.11	$nmol\,m^{-3}$
Propionate	µM	11	0.88	0.35	1.36	0.06	0.01	0.11	$nmol\,m^{-3}$
Adipate	µM	11	0.09	< LOD	0.24	0.04	0.04	0.01	$nmol\,m^{-3}$
Salicylate	µM	11	0.06	< LOD	0.15	0.04	0.04	0.006	$nmol\,m^{-3}$
Benzoate	µM	11	0.06	< LOD	0.15	0.02	0.02	0.005	$nmol\,m^{-3}$
Pinate	µM	11	0.009	< LOD	0.03	0.01	0.01	0.0005	$nmol\,m^{-3}$
Azelate	µM	11	0.02	< LOD	0.09	0.03	0.03	0.0009	$nmol\,m^{-3}$
All Organic Acids	µM	11	379	138	1000	–	–	19.0	$nmol\,m^{-3}$

ACPD
15, 24871–24908, 2015

Table 2. Chemical formulae and possible structures of organic components identified via HPLC-(-)-ESI-HR-ToF-MS within BYI fog water samples. Formulae with multiple isomers (different retention times) are marked with an asterisk (*). Multiple plausible formulae were identified for species prefixed with "e.g.". Only species with mass spectral abundances ≥ 500 a.u. were included.

m/z^-	Formula (M)	Difference (ppm)	t_R (min)	Abund. (a.u.)	Possible identification
85.0311	$C_4H_6O_2$	−18.2	3.18	11 000	Methacrylic acid
105.0367			9.32	1200	
113.027	$C_5H_6O_3$	−22.32	3.67	500	Oxo-pentenoic acid
117.0565	$C_5H_{10}O_3$	−6.72	4.54	1700	Hydroxy-pentanoic acid*
117.057	$C_5H_{10}O_3$	−10.63	3.43	6900	Hydroxy-pentanoic acid*
121.0306	$C_7H_6O_2$	−9.34	9.82	1700	Hydroxy-benzaldehyde
127.0415	$C_6H_8O_3$	−11.58	5.79	990	Oxo-hexeneoic acid
129.0206	$C_5H_6O_4$	−9.72	3.67	800	Pentenedioic acid*
129.021	$C_5H_6O_4$	−22.33	3.18	600	Pentenedioic acid*
129.057	$C_6H_{10}O_3$	−1.11	5.96	2100	Methyl-oxo-pentanoic acid*
129.0571	$C_6H_{10}O_3$	−10.78	7.00	2700	Methyl-oxo-pentanoic acid*
131.0362	$C_5H_8O_4$	−9.57	3.18	6100	Methyl-succinic acid
131.0362	$C_5H_8O_4$	−9.34	4.34	11 000	Glutaric acid
131.0727	$C_6H_{12}O_3$	−10.13	9.82	1100	Hydroxy-Hexanoic acid*
131.073	$C_6H_{12}O_3$	−12.18	7.95	1800	Hydroxy-Hexanoic acid*
137.0255	$C_7H_6O_3$	−8.18	16.17	6900	Salicylic acid
138.0207	$C_6H_5NO_3$	−7.4	13.18	39 100	4-Nitrophenol
143.0359	$C_6H_8O_4$	−6.53	3.18	21 000	Hexenedioic acid*
143.0374	$C_6H_8O_4$	−16.85	6.86	2700	Hexenedioic acid*
143.0729	$C_7H_{12}O_3$	−10.47	11.43	1000	Methyl-pentenedioic acid
145.0513	$C_6H_{10}O_4$	−4.54	8.93	1200	Methyl-glutaric acid*
145.0515	$C_6H_{10}O_4$	−5.98	7.10	1900	Adipic acid
145.052	$C_6H_{10}O_4$	−9.04	9.52	2700	Methyl-glutaric acid*
149.0258	$C_8H_6O_3$	−9.29	9.32	3200	Formyl-benzoic acid
152.0358	$C_7H_7NO_3$	−3.3	17.85	1500	Methyl-nitrophenol
152.0365	$C_7H_7NO_3$	−7.9	19.33	7900	2-Methyl-4-nitrophenol
154.0164	$C_6H_5NO_4$	−11.95	10.46	2700	Nitroguaiacol
157.052	$C_7H_{10}O_4$	−8.5	6.32	2900	Heptenedioic acid*
157.053	$C_7H_{10}O_4$	−14.71	5.22	1100	Heptenedioic acid*
159.0676	$C_7H_{12}O_4$	−8.35	10.79	1400	Pimelic acid
163.0416	$C_9H_8O_3$	−9.22	12.63	1100	Previously identified (Desyaterik et al., 2013)
165.0205	$C_8H_6O_4$	−7.2	10.13	31 300	Phthalic acid
165.0211	$C_8H_6O_4$	−11.59	12.06	2300	Benzenedicarboxylic acid
166.0525	$C_8H_9NO_3$	−8.98	23.61	3000	Dimethyl-nitrophenol
171.0673	$C_8H_{12}O_4$	−5.88	8.33	2900	Octenedioic acid*
171.0683	$C_8H_{12}O_4$	−11.71	6.95	1700	Octenedioic acid*
171.9831			19.71	2700	
173.0467	$C_7H_{10}O_5$	−6.39	4.22	3200	Isoprene photooxidation product (Nguyen et al., 2011)
179.0368	$C_9H_8O_4$	−10.26	15.23	3700	Phthalic acid, methyl ester
181.0162	$C_8H_6O_5$	−11.01	5.65	1300	Hydroxy-benzene-dicarboxylic acid*
181.0162	$C_8H_6O_5$	−10.71	8.81	1200	Hydroxy-benzene-dicarboxylic acid*
181.019	$C_5H_{10}O_5S$	−8.7	2.82	1900	Previously identified (Nguyen et al., 2014a)

ACPD
15, 24871–24908, 2015

Table 2. Continued.

m/z^-	Formula (M)	Difference (ppm)	t_R (min)	Abund. (a.u.)	Possible identification
182.0117	$C_7H_5NO_5$	−11.77	18.75	990	Carboxy-nitrophenol
182.9989	$C_4H_8O_6S$	−10.81	1.92	6700	
183.0065	$C_6H_4N_2O_5$	−9.43	15.08	11 000	2,4-Dinitrophenol
185.0833	$C_9H_{14}O_4$	−7.62	13.54	2300	Pinic acid*
185.0841	$C_9H_{14}O_4$	−11.55	9.70	2000	Nonenedioic acid*
187.0631	$C_8H_{12}O_5$	−10.1	5.10	1200	Alpha-pinene oxidation product (Claeys et al., 2009)*
187.0635	$C_8H_{12}O_5$	−12.35	7.76	1600	Alpha-pinene oxidation product*
189.078	$C_8H_{14}O_5$	−6.03	6.54	1300	Diaterpenylic acid; known oxidation product of alpha-pinene (Yasmeen et al., 2010)
195.0343	$C_6H_{12}O_5S$	−5.4	6.17	1200	
195.0347	$C_6H_{12}O_5S$	−7.33	7.00	2000	
197.0216	$C_7H_6N_2O_5$	−5.87	21.23	1300	Methyl-dinitrophenol
201.0788	$C_9H_{14}O_5$	−9.87	10.74	1200	Alpha-pinene oxidation product (Kahnt et al., 2013)
203.0582	$C_8H_{12}O_6$	−10.03	8.75	2300	Methyl-butane-tricarboxylic acid (MBTCA); gas-phase pinonic acid oxidation product (Szmigielski et al., 2007b)
211.0305	$C_6H_{12}O_6S$	−11.1	7.40	1300	
211.0306	$C_6H_{12}O_6S$	−11.09	6.86	1200	
211.031	$C_6H_{12}O_6S$	−13.18	9.40	3000	
225.0093	$C_6H_{10}O_7S$	−8.16	2.50	2300	Methylglyoxal oxidation product (Sareen et al., 2010)
228.0214	$C_8H_7NO_7$	−28.14	12.97	900	Oxygenated nitrophenol
239.0249	$C_7H_{12}O_7S$	−7.57	4.10	1200	1,3,5-trimethylbenzene oxidation product (Praplan et al., 2014)
239.0482			21.56	3500	
241.0048	$C_6H_{10}O_8S$	−9.92	2.18	2800	
253.0419	$C_8H_{14}O_7S$	−9.69	7.59	800	Limonene oxidation product (Nguyen et al., 2014a; Surratt et al., 2008)*
267.0567	$C_9H_{16}O_7S$	-8.69	10.55	1800	Limonene oxidation product (Nguyen et al., 2014; Mazzoleni et al., 2010)*
267.0576	$C_9H_{16}O_7S$	−12.47	10.85	600	Limonene oxidation product (Nguyen et al., 2014; Mazzoleni et al., 2010)*
267.0579	$C_9H_{16}O_7S$	−12.94	9.92	850	Limonene oxidation product (Nguyen et al., 2014; Mazzoleni et al., 2010)*
267.0579	$C_9H_{16}O_7S$	−13.64	11.00	500	Limonene oxidation product (Nguyen et al., 2014; Mazzoleni et al., 2010)*
269.0363	$C_8H_{14}O_8S$	−9.98	7.44	500	
284.0473	$C_{11}H_{11}NO_8$	−21.51	14.96	600	
294.0677	$C_{10}H_{17}NO_7S$	−8.07	24.87	7800	Monoterpene oxidation product (Surratt et al., 2008)*
294.068	$C_{10}H_{17}NO_7S$	−9.2	26.71	7600	Monoterpene oxidation product*
297.0601	e.g., $C_{17}H_{14}O_3S$	−10.86	8.87	700	
310.0631	$C_{10}H_{17}NO_8S$	−9.35	19.56	600	Monoterpene oxidation product (Mazzoleni et al., 2010; Surratt et al., 2008)*
333.0208	$C_{14}H_{10}N_2O_6S$	−6.23	20.65	700	
361.1649	$C_{15}H_{26}N_2O_8$	−8.83	12.32	500	
497.3325	$C_{23}H_{50}N_2O_7S$	−11.74	16.74	600	
514.3221	$C_{22}H_{49}N_3O_8S$	−10.35	16.74	1600	
635.3506	e.g., $C_{26}H_{56}N_2O_{13}S$	−11.82	18.46	5900	

ACPD
15, 24871–24908, 2015

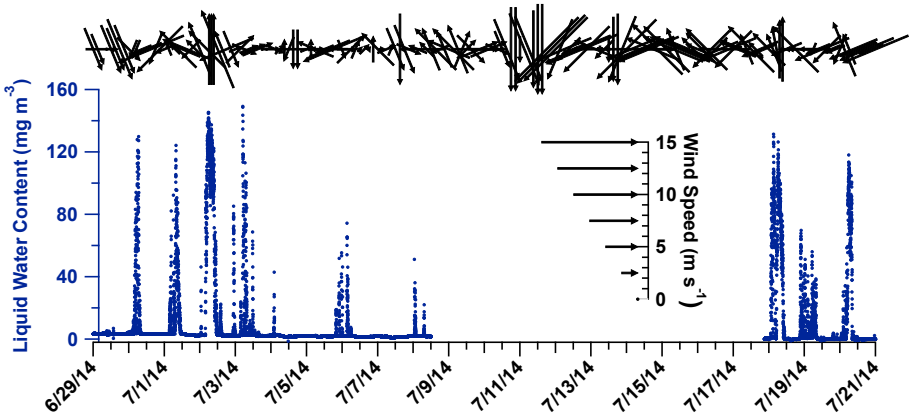

Figure 1. Wind speed and direction during fog sampling period, shown as vector arrows (top): speed is displayed as the length of each arrow and direction is displayed as tilt, pointing away from wind origin. LWC measured during the entire study period is shown in blue along the bottom of the plot. Fog was not collected in mid-July during the monsoonal period.

ACPD
15, 24871–24908, 2015

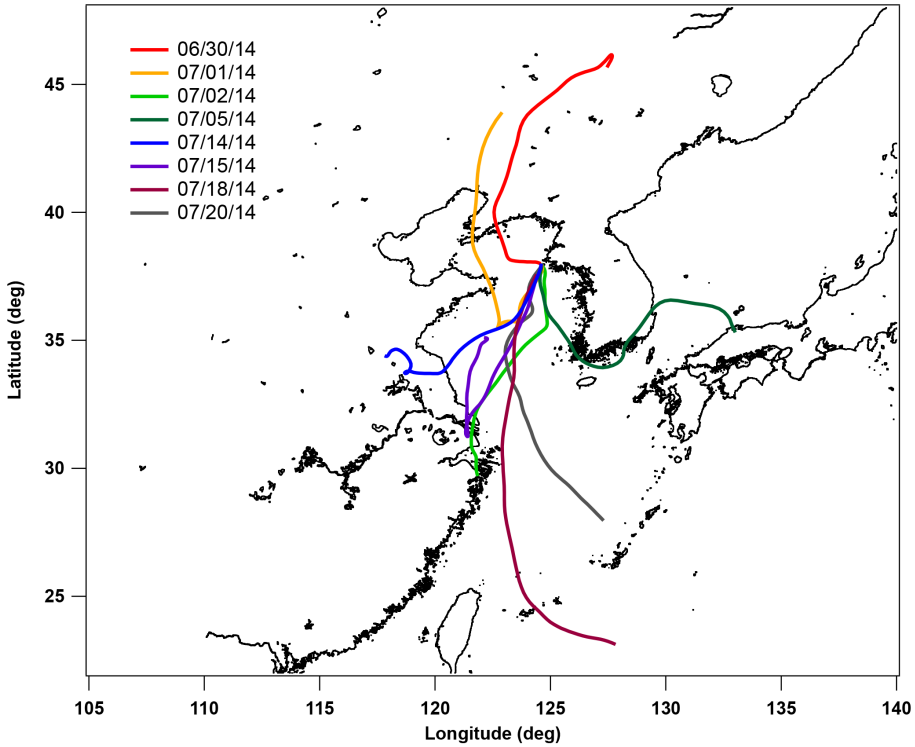

Figure 2. Back trajectories of air masses intercepted during fog events (72 h at one hour time resolution; HySPLIT). Each trajectory was initiated at the approximate beginning of a fog event.

ACPD
15, 24871–24908, 2015

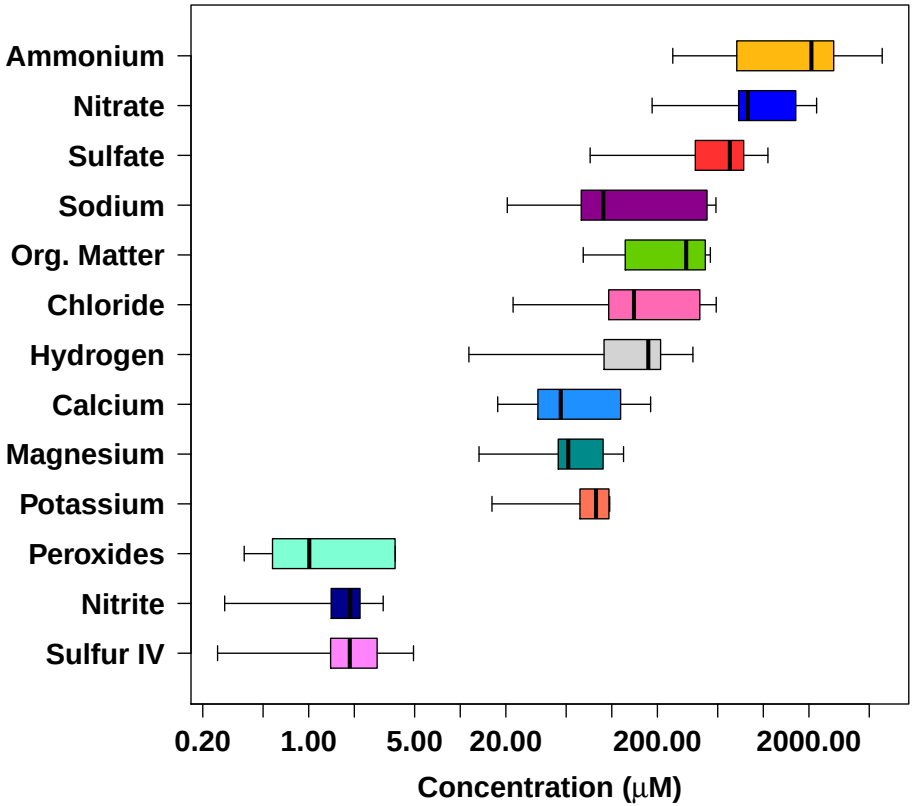

Figure 3. Concentrations of major components quantified in BYI fog samples. Boxes show 25th and 75th percentiles with the median bar in the center, and whiskers show 10th and 90th percentiles. Total organic matter was calculated from measured TOC using a ratio of 1.8 g/1.0 g OM/OC (Zhang et al., 2005) and an estimated mean molecular mass of 100 g mol^{-1}. Note that for most ions, $N = 14$, for pH, S(IV) and peroxides, $N = 11$, for formaldehyde, $N = 10$, and for total organic matter, $N = 8$.

ACPD
15, 24871–24908, 2015

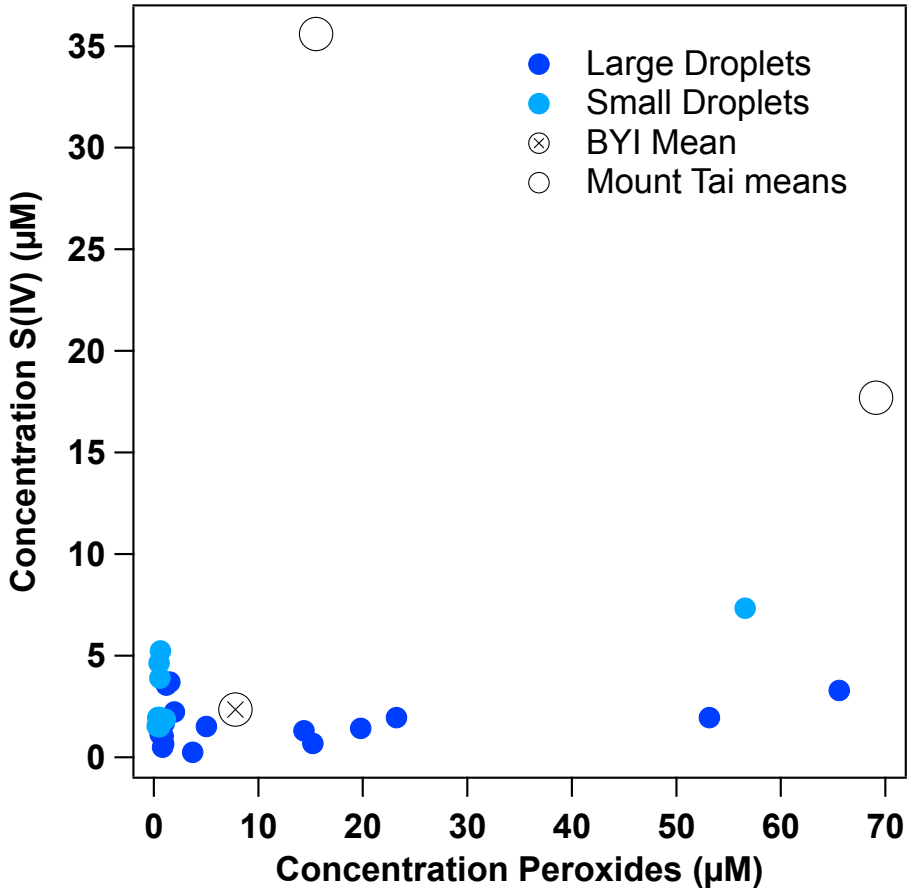

Figure 4. Droplet size-segregated concentrations of S(IV) and peroxides quantified in BYI fog samples. S(IV) concentrations were low in BYI fog as compared to those measured at Mount Tai (summer 2007 and 2008; Shen et al., 2012). For both species, $N = 11$.

ACPD
15, 24871–24908, 2015

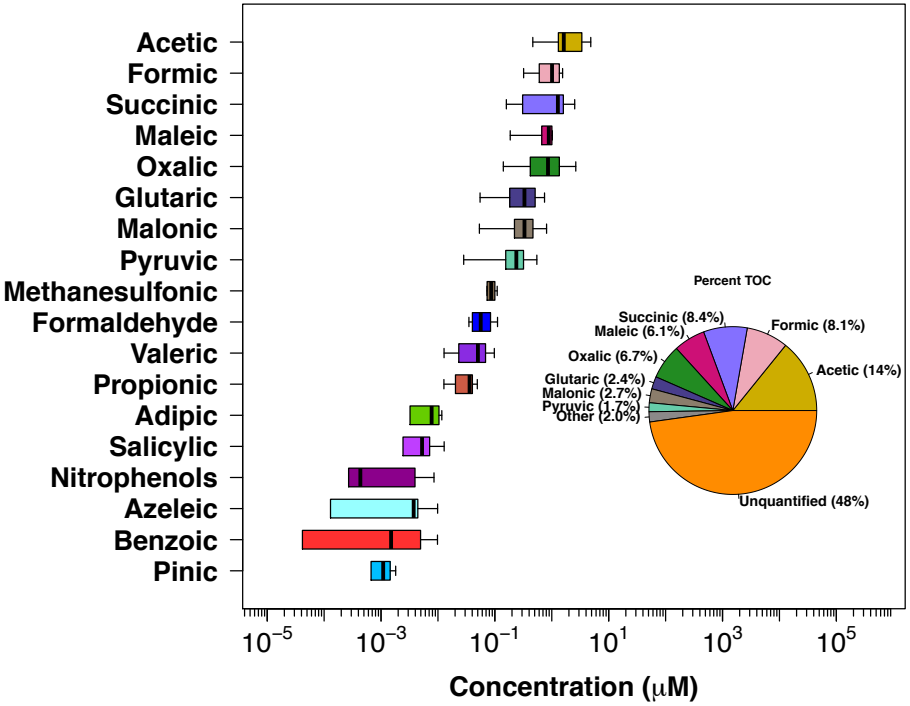

Figure 5. Concentrations of major carbonaceous components quantified in BYI fog samples. Box-and-whisker plot shows 25th and 75th percentiles with the median bar in the center, and whiskers at the 10th and 90th percentiles. Note that for C_1–C_5 organic acids, $N = 11$, for formaldehyde, $N = 10$, and for components with C_6 or greater, $N = 11$. Pie chart shows carbonaceous composition as a percentage of TOC (only those samples with results from all organic analyses included, $N = 7$).

ACPD
15, 24871–24908, 2015

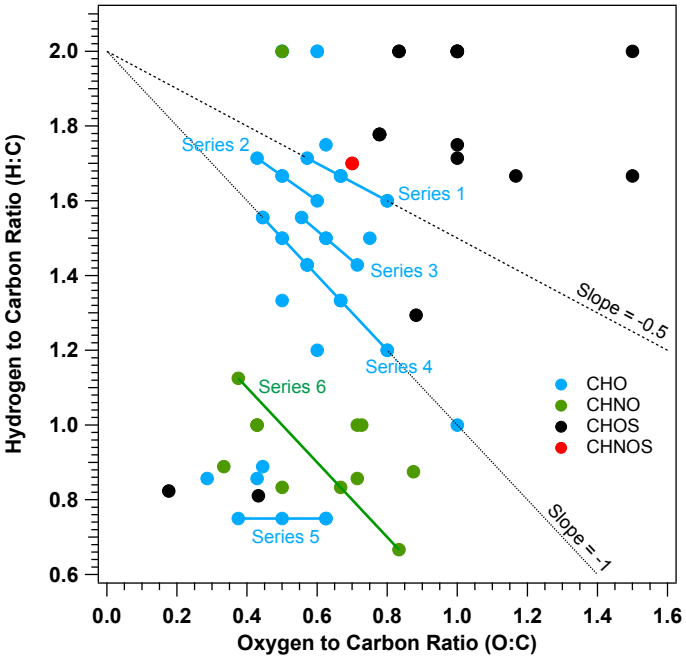

Figure 6. Polar organic compounds identified within fog samples using HPLC-(-)-ESI-HR-ToF-MS detection illustrated via a van Krevelen diagram. Colors represent groupings of compounds by elemental composition; solid lines show homologous series of di-carboxylic acids (blue, series 1–5) and nitrophenols (green, series 6); dashed grey lines show slopes typical of samples in previous studies (Chen et al., 2015) of −0.5 for remote/rural (top) and −1 for urban (bottom).

ACPD
15, 24871–24908, 2015

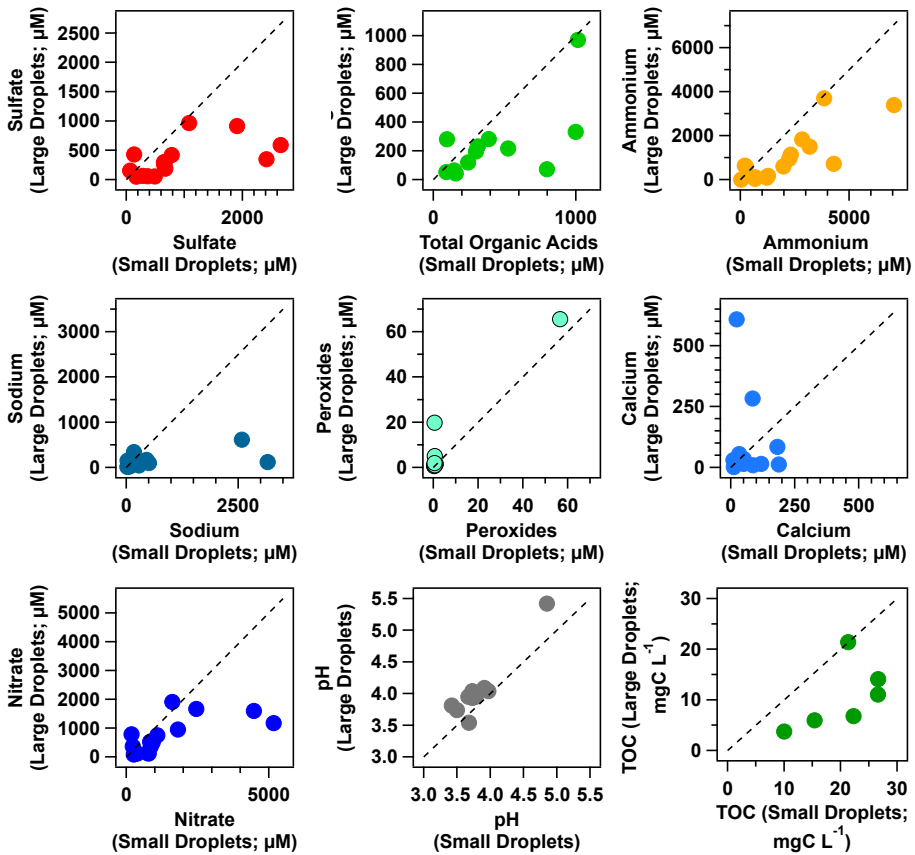

Figure 7. Scatter plots showing size distribution of major species in BYI fog water samples. All species shown, with the exception of peroxides, were enriched in small droplets.

ACPD
15, 24871–24908, 2015